


RESEARCH

Open Access



Single cell analysis identified a basal cell transition state associated with the development and progression of bladder cancer

Yang Li^{1,2†}, Pengjie Shi^{1,2}, Yuhong Ding^{1,2}, Zhipeng Yao^{1,2}, Lilong Liu^{1,2}, Junyi Hu^{1,2}, Zhenghao Liu^{1,2}, Jinxu Li^{1,2}, Ke Chen^{1,2*} and Yaxin Hou^{1,2*} 

Abstract

Background Bladder cancer (BC) is a prevalent malignancy characterized by significant cellular heterogeneity. While single-cell multi-omics studies have provided valuable insights, much of the existing data remains underexplored, limiting our understanding of BC's molecular mechanisms. Uncovering the pathogenesis of BC and finding new treatment methods are urgent problems to be solved. This study aims to address this gap by re-analyzing available single-cell datasets to uncover novel insights into BC.

Methods In this study, we retrieved three single-cell transcriptome datasets by searching the Gene Expression Omnibus (GEO) database, focusing on single-cell sequencing of normal mouse bladder within the past 5 years. Through quality control and batch effect elimination, we obtained a total of 24,930 cells including epithelial, stromal, and immune cells. Subgroup analysis, pseudotemporal analysis, cell–cell communication, and transcription factor analysis were conducted specifically on epithelial cells to identify a transitional state during basal cell differentiation. We further compared the expression profiles of key transcription factors in cancer and normal tissues. In addition, we also performed immunohistochemical staining and survival analysis for key transcription factors.

Results Subgroup analysis revealed multiple subtypes of epithelial cells, including basal, umbrella, and intermediate cells. Through pseudotemporal analysis, we discovered the developmental trajectory from basal cells to umbrella cells and further found that Basal_I is a transitional state for basal cell differentiation. Cell-to-cell communication analyses highlighted the pivotal role of Basal_I in cell–cell interactions, and key ligand–receptor pairs associated with cancer progression were also identified. Furthermore, elevated expression levels of key transcription factors in Basal_I were found to be closely associated with the stage and prognosis of BC. Immunohistochemical staining results further confirmed the upregulated expression of these transcription factors in BC.

[†]Yang Li, Pengjie Shi, Yuhong Ding and Zhipeng Yao contributed equally to this work.

*Correspondence:

Ke Chen

shenke@hust.edu.cn

Yaxin Hou

18351033626@163.com

Full list of author information is available at the end of the article



© The Author(s) 2024. **Open Access** This article is licensed under a Creative Commons Attribution-NonCommercial-NoDerivatives 4.0 International License, which permits any non-commercial use, sharing, distribution and reproduction in any medium or format, as long as you give appropriate credit to the original author(s) and the source, provide a link to the Creative Commons licence, and indicate if you modified the licensed material. You do not have permission under this licence to share adapted material derived from this article or parts of it. The images or other third party material in this article are included in the article's Creative Commons licence, unless indicated otherwise in a credit line to the material. If material is not included in the article's Creative Commons licence and your intended use is not permitted by statutory regulation or exceeds the permitted use, you will need to obtain permission directly from the copyright holder. To view a copy of this licence, visit <http://creativecommons.org/licenses/by-nc-nd/4.0/>.

Conclusions Collectively, we found a transitional state of basal cells in normal bladder epithelial cells in mice, which may be related to the occurrence and development of BC, providing important clues for further understanding of the pathogenesis of BC. Our study provided possible molecular mechanisms or target for the research and treatment of BC.

Keywords Bladder cancer, scRNA-seq, Basal cell

Background

Although human has made great progress in medicine, there are still many unsolved problems, such as cancer [1–3]. Cancer is a pathological condition characterized by the uncontrolled proliferation of abnormal cells, often leading to local invasion and metastasis. It arises from genetic mutations and is influenced by environmental and lifestyle factors, affecting a wide range of tissues and organs. Numerous research studies on cancer continue to emerge [4–7].

Current cancer therapies remain limited in effectiveness and often come with significant side effects. Research efforts are largely focused on improving existing treatments like chemotherapy, which targets rapidly dividing cells, and immunotherapy, which aims to enhance the immune system's ability to recognize and destroy cancer cells [8–10]. Despite these advancements, there is still a need for more targeted, less toxic options to improve patient outcomes and address the complexities of different cancer types.

Bladder cancer is one of the most prevalent malignancies of the urinary tract, representing a significant public health challenge worldwide. It ranks among the top 10 most common cancers worldwide, with an estimated 82,290 new cases and 19,870 deaths in 2023 [11]. The disease is characterized by its high recurrence rate and propensity for progression, necessitating lifelong surveillance and treatment, which contribute to substantial healthcare costs and patient morbidity [12]. The majority of bladder cancers are urothelial carcinomas, originating from the epithelial lining of the bladder. Clinically, bladder cancer presents in two primary forms: non-muscle-invasive bladder cancer (NMIBC) and muscle-invasive bladder cancer (MIBC) [13]. NMIBC accounts for approximately 75% of cases at initial diagnosis and is confined to the mucosa or submucosa. It is typically managed with transurethral resection and intravesical therapies. However, NMIBC exhibits a high recurrence rate and can progress to MIBC, which is more aggressive and associated with a poorer prognosis. MIBC requires radical treatments such as cystectomy, chemotherapy, and, in some cases, radiation therapy [14]. Despite advancements in surgical techniques and the advent of immunotherapies, the molecular mechanisms underlying bladder cancer

initiation, progression, and metastasis remain incompletely understood [15, 16]. Gaining deeper insights into the cellular composition and molecular pathways involved in normal bladder function and cancer development is critical for enhancing diagnostic, prognostic, and therapeutic strategies.

Normal bladder epithelium, also known as urothelium, comprises three main cell types: basal cells, intermediate cells, and umbrella cells [17]. The differentiation and maintenance of these cell types are tightly regulated by various signaling pathways and transcription factors. Disruption of these regulatory mechanisms can lead to pathological conditions, including cancer.

Single-cell RNA sequencing (scRNA-seq) has emerged as a powerful tool to dissect cellular heterogeneity and uncover molecular signatures at single-cell resolution [18, 19]. This technology allows for the identification of rare cell populations and the mapping of developmental trajectories, offering invaluable insights into tissue biology and disease mechanisms [20–23]. Despite numerous studies on single-cell multi-omics in bladder cancer, most of the data remains underutilized [24–28].

In this study, we employ scRNA-seq to comprehensively analyze the normal mouse bladder epithelium, aiming to delineate the distinct cell populations and their transcriptional profiles. We gathered three single-cell transcriptome datasets from literature and public databases [29, 30]. This comprehensive analysis provides a detailed map of the cellular landscape in the normal mouse bladder, laying the groundwork for understanding the molecular alterations that drive bladder cancer. By integrating single-cell transcriptomics and functional assays, we aim to uncover key regulatory mechanisms and potential therapeutic targets that could inform future strategies for bladder cancer treatment and management.

Materials and methods

Patients and samples

All bladder cancer samples were obtained from bladder cancer patients in the Tongji Hospital of Tongji Medical College, Huazhong University of Science and Technology, Wuhan, China. All procedures were approved by the Institutional Review Board of Tongji Medical College, Huazhong University of Science and Technology.

Animals and model establishment

All animal procedures were approved by the Animal Care and Use Committee of Tongji Medical College of Huazhong University of Science and Technology. Wild-type (WT) C57BL/6J male mice (6–8 week old) was purchased from Beijing Vital River Laboratory Animal Technology Co., Ltd. The mouse orthotopic bladder cancer model was constructed based on a previous study [31]. The mice were anesthetized with isoflurane inhalation, and a 0.5 cm incision was made in the midline of the lower abdomen of the mice to find the bladder. MB49 cell suspension (0.1 ml, density of 1×10^6 cells/ml) was orthotopically injected into the bladder through a syringe. Mice were allowed to recover from anesthesia in a small recovery room before returning to the housing facility. After being observed for blood in the urine, the mice died.

IHC staining assay

The 4 μ m sections obtained from BC patients and orthotopic tumors of WT were deparaffinized by heating at 60 °C for 30 min, followed by three washes with xylene, each lasting 10 min. The sections were then rehydrated by sequentially washing for 5 min in absolute ethanol I, absolute ethanol II, 85% alcohol, 75% alcohol, and distilled water. Antigen retrieval was performed using a microwave oven to heat the samples in a citric acid antigen retrieval buffer (pH 6.0). To block endogenous peroxidase activity, the sections were incubated with 3% hydrogen peroxide for 30 min. This was followed by a 30-min incubation at room temperature with 3% BSA to block nonspecific binding. The tissue sections were then incubated overnight at 4 °C in a wet box with primary antibodies anti-JUN, anti-EGR1, anti-NR3C1, anti-NFIX, or anti-GATA6. Immunodetection was carried out at room temperature using HRP anti-Rabbit IgG antibody and DAB color developing solution. Finally, the sections were scanned as high-resolution digital images at 5.4 \times using a Panoramic MIDI II scanner.

The expression levels of JUN/EGR1/NR3C1/NFIX/GATA6 were evaluated using Remmele and Stegner's semiquantitative immunoreactive score scale [32]. The staining intensity was scored from 0 to 3 (0: negative; 1: weak; 2: moderate; 3: strong). The proportion of positive cells was also scored: 0 (no staining), 1 (1–25%), 2 (26–50%), 3 (51–75%), and 4 (76–100% stained cells). The final score was obtained by multiplying the staining intensity score by the positive cell proportion score.

Quality control and cell-type identification

The QC process was conducted using Seurat (version 4.3.0) [33]. Single cells were deemed low-quality and

excluded if they had fewer than 400 UMIs, more than 5000 UMIs, or over 20% mitochondrial-derived UMI counts. The DoubletFinder package (version 2.0.3) was employed to identify doublets [34]. The neighborhood size (pK) was calculated using the mean–variance-normalized bimodality coefficient (BCMVN) of each sample, and the number of artificial doublets (pN) was set to 0.25. Harmony was used to correct batch effects among the patients, utilizing the top 30 principal components and the top 2000 variable genes [35]. Main cell clusters were then identified with Seurat's FindClusters function (resolution=0.8) and visualized using 2D UMAP [36]. The FindAllMarkers function was utilized to identify the markers for each cell cluster.

Enrichment analysis

Identify DEGs using Seurat's FindMarkers function. Use the following truncation thresholds: $\text{adj.pval} < 0.01$ and $|\log_2\text{Foldchange}| > 1.5$. These DEGs were then loaded into the clusterProfiler for GO enrichment analysis and $\text{adj.pval} < 0.05$ was considered to be significantly enriched [37].

Trajectory inference and analysis

Monocle3 was used to perform pseudotime analysis to find relationships among epithelial subtypes [38]. With differentialGeneTest function, the following parameters were set: $\text{mean expression} \geq 0.125$, $\text{num_cells_expressed} \geq 10$, $\text{qval} < 0.01$.

Cell–cell communication analysis

Cell–cell communication analysis was conducted by CellChat (version 1.6.1) [39]. All thresholds are default values. Ligands and receptors in above 10 percent of cells were then analyzed, and only p value < 0.01 was retained for predicting cell–cell interaction.

Statistical analyses

All statistical analyses and graph generation were performed in R (version 4.3.2) and GraphPad Prism (version 9.0).

Results

Construct a single-cell transcriptomic landscape of normal mouse bladder

We gathered three single-cell transcriptome datasets from literature and public databases, focusing on the normal mouse bladder. Following rigorous quality control measures and the elimination of duplicate cells, a comprehensive set of 24,930 cells was assembled (Fig. 1A). These datasets comprised 15,118, 4845, and 4967 cells, respectively. By employing the Harmony algorithm, we effectively mitigated batch effects and executed the initial

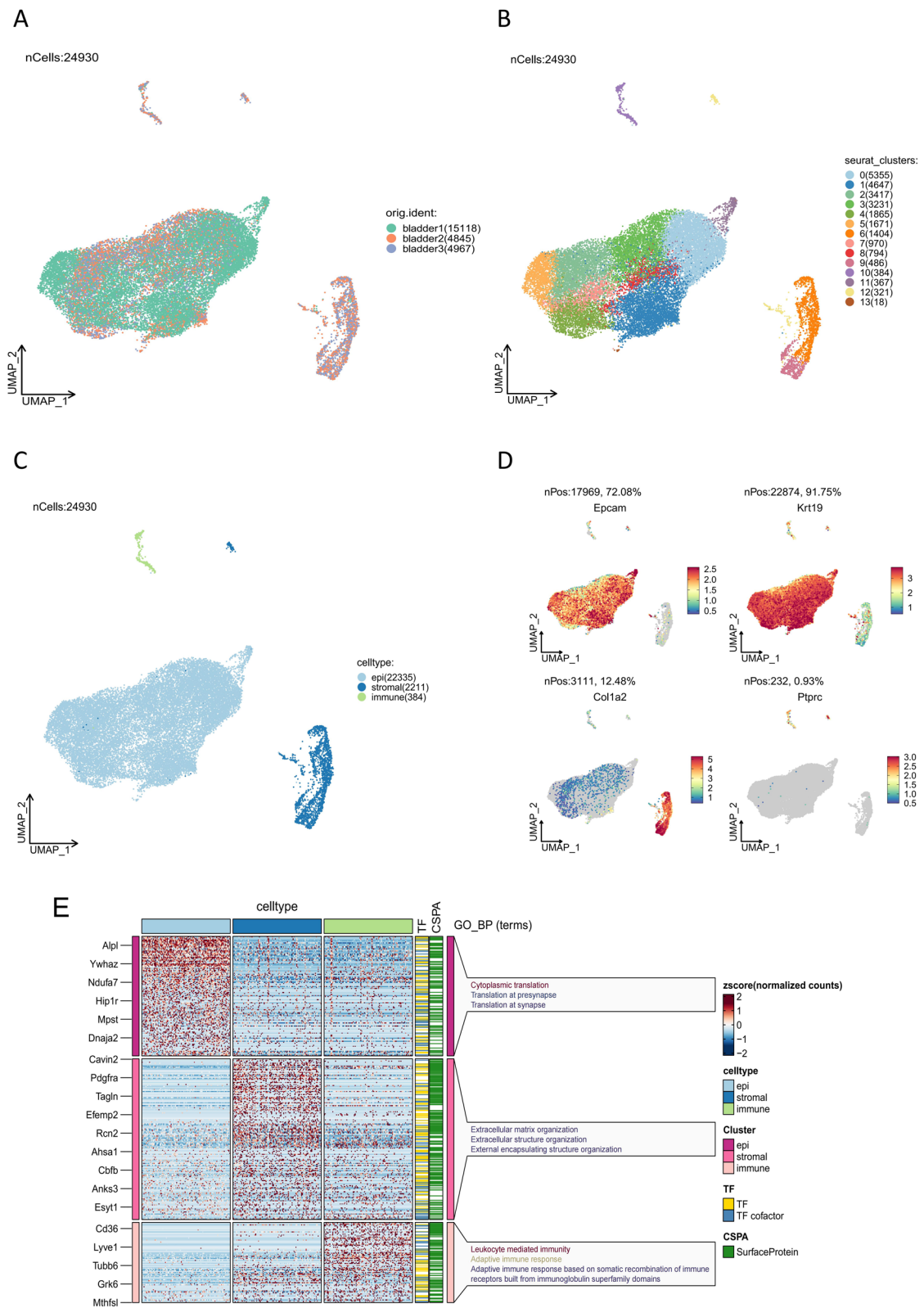


Fig. 1 Construction of single-cell transcriptome profiles of the normal mouse bladder. **A** UMAP plot of all cells grouped by original datasets. **B** UMAP plot of all cells grouped by seurat_clusters. **C** UMAP plot of all cells grouped by major cell types. **D** Feature plot of markers used to annotate major cell types. **E** Heatmap of DEGs of every cell types and GO enriched pathways. DEGs differentially expressed genes, GO gene ontology

dimensionality reduction clustering, culminating in the identification of 14 distinct clusters (Fig. 1B). According to the markers used in the literature, we accurately classified these clusters into epithelial (22,335 cells, Epcam, Krt19), stromal (2211 cells, Col1a2, Acta2), and immune (384 cells, Ptpcr) populations, each demonstrating unique transcriptional signatures [40, 41] (Fig. 1C, D).

Subsequent gene ontology (GO) enrichment analyses unveiled profound insights into the functional characteristics of these cell types (Fig. 1E). Specifically, epithelial cells were enriched in pathways associated with cytoplasmic transport, while stromal cells displayed enrichment in pathways pertaining to extracellular matrix organization and extracellular structure organization. Immune cells, in contrast, showcased enrichment in pathways linked to lymphocyte-mediated immune response and adaptive immune response, consistent with their respective cellular functions and previous studies [30]. These findings not only confirm the accuracy of our cell type annotation but also provide valuable insights into the functional diversity within the normal mouse bladder transcriptome.

Cluster epithelial cells into multiple subtypes

Following the isolation of epithelial cells, we further categorized them into distinct subtypes based on traditional markers, namely basal cells (characterized by Krt5, Trp63), umbrella cells (marked by Upk2, Upk3a), and intermediate cells occupying transitional states [29, 30] (Fig. 2A). This segmentation resulted in 13 discrete epithelial subtypes, comprising 6 basal cell subtypes, 4 umbrella cell subtypes, and 3 intermediate cell subtypes, each exhibiting a distinct transcriptional landscape (Fig. 2B).

GO enrichment analysis revealed functional differences among these subtypes (Fig. 2C). Notably, Basal_I, Basal_III, and Basal_IV were enriched in pathways related to RNA splicing, mRNA processing, and DNA replication, highlighting their involvement in fundamental cellular processes. Conversely, Basal_II and Basal_V exhibited enrichment in cytoplasmic transport pathways, while Basal_VI featured marker genes associated with cellular respiration. Umbrella cells emerged as pivotal players in oxidative phosphorylation and cell–cell junction organization, underscoring their role in bladder epithelial function.

Of particular interest, the Basal_I subtype exhibited heightened expression of the Chka gene, responsible for encoding choline kinase α —an enzyme pivotal in catalyzing the initial step of phosphatidylcholine synthesis, critical for membrane biogenesis [42] (Fig. 2D). Meanwhile, the Basal_III subtype showcased elevated expression of the Lig1 gene, encoding DNA ligase I, which is crucial

for DNA repair and replication [43]. The Basal_IV subtype displayed enhanced expression of the Cenpf gene, responsible for encoding centromere protein F, vital for cell mitosis and centromere structure maintenance [44]. Collectively, these findings suggest the proliferative and stem cell-like properties inherent in the Basal_I, Basal_III, and Basal_IV subpopulations, shedding light on their potential roles in bladder epithelial homeostasis and regeneration.

Pseudotemporal and SCENIC analysis identified Basal_I as transitional basal cell

Our pseudo-temporal analysis of all epithelial cell subtypes using Monocle3 revealed a developmental trajectory from basal cells to intermediate cells and ultimately to umbrella cells, consistent with previous studies (Fig. 3A, B). Specifically, Basal_IV subtype occupies the initial stage of this developmental trajectory, which subsequently transitions through Basal_I, Basal_II, Basal_III, and Basal_V subtypes, followed by three states of intermediate cells, before finally differentiates into four umbrella cell subtypes. Thus, Basal_I serves as an intermediate transition state in the differentiation of basal cells into intermediate cells and umbrella cells. The 3D pseudo-temporal analysis corroborated these findings (Fig. 3C). In terms of cell density, Basal_IV exhibited the highest density at the beginning, and the density of Basal_I, Basal_II, Basal_III and Basal_V subtypes gradually increased and then decreased. The intermediate cells exhibited a similar pattern, while the umbrella cells showed a gradual increase in density toward the end (Fig. 3D).

We then extracted the genes contributing to the epithelial pseudotime series analysis for cluster analysis, resulting in four distinct gene expression clusters (Fig. 3E). The expression of genes in cluster 1 gradually increased with pseudotime, the expression of genes in cluster 2 gradually decreased with pseudotime, and the expression of genes in cluster 3 first increased with pseudotime and then gradually decreased. The genes in cluster 4 were initially highly expressed, then decreased, before gradually returning to baseline levels.

Further analysis of transcription factors (TFs) revealed three distinct clusters (Fig. 3F). TFs in cluster 1 were highly expressed at the beginning of the pseudotime, then decreased, and finally increased. TFs in cluster 2 were gradually increased and TFs in cluster 3 were gradually decreased at pseudo time. Performing GO enrichment analysis of the three clusters of transcription factors, we found that cluster 3, whose expression gradually decreased with pseudotime, was mainly related to pathways related to mRNA metabolism regulation, regulation of DNA-binding transcription factor activity,

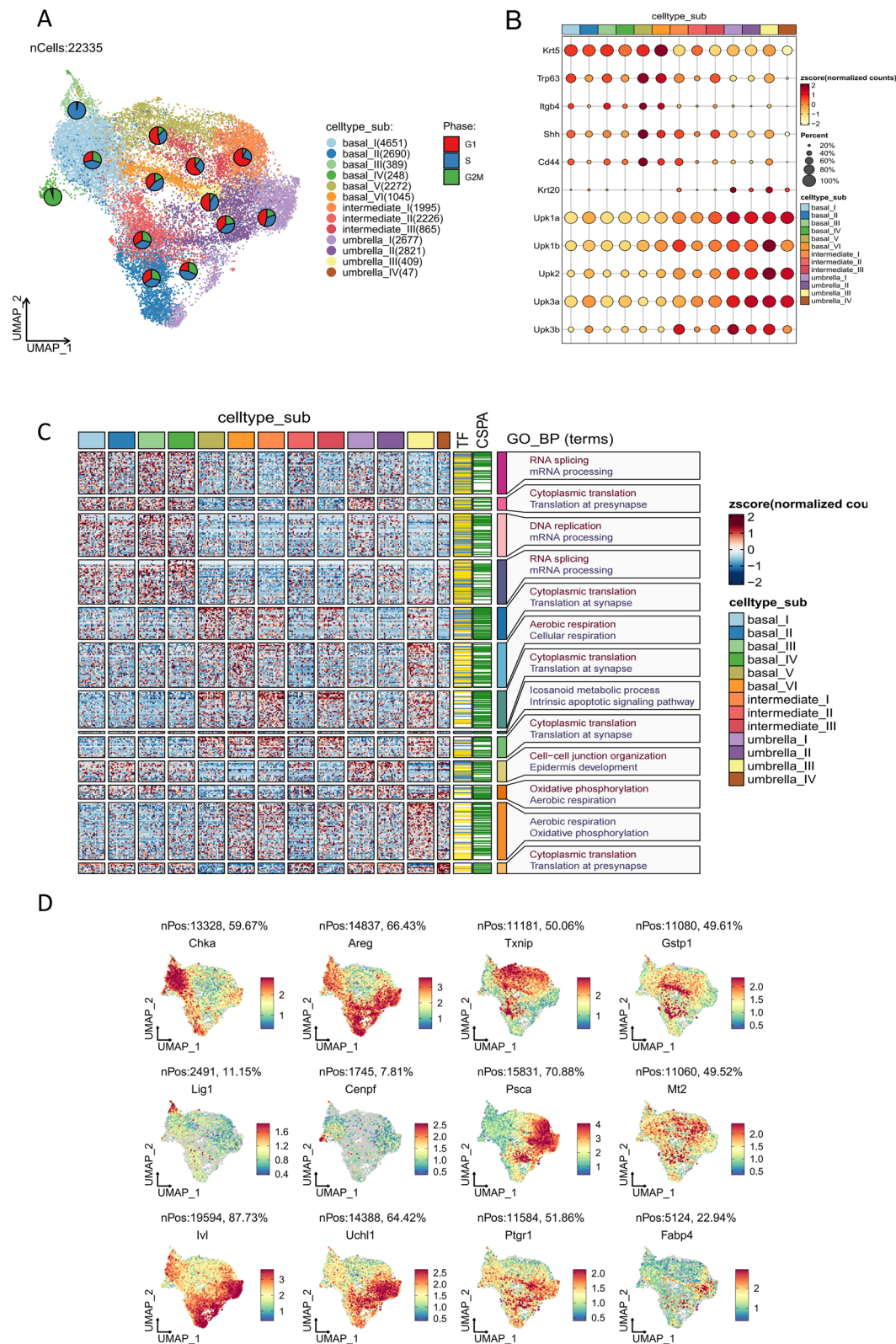


Fig. 2 Cluster epithelial cells into multiple subtypes. **A** UMAP plot of epithelial cell grouped by subtypes. **B** Dot plot of markers used to annotate subtypes. **C** Heatmap of DEGs of subtypes and GO enriched pathways. **D** Feature plot of top markers expressed by subtypes. DEGs differentially expressed genes, GO gene ontology

miRNA transcription, chromatin remodeling and maintenance of cell population (Fig. 3G). In contrast, cluster 2, whose expression gradually increased over pseudo time, was mainly associated with pathways related to muscle cell differentiation and gland development. Notably, six transcription factors in cluster 3—Gata6, Nr3c1, Klf9, Egr1, Jun and Nfix—were highly expressed in Basal_I, with their expression gradually declining as pseudotime progressed (Fig. 3H, I). SCENIC analysis of epithelial cell subsets was also performed, which revealed higher levels of activity of Gata6, Klf9, and Nr3c1 in Basal_I compared to other subtypes (Fig. 3J). In conclusion, Basal_I represents an intermediate transition state in the differentiation of basal cells into intermediate cells and umbrella cells.

Basal_I subtype dominated the interaction with other subtypes

In our comprehensive analysis, cell communication assessment using CellChat across all epithelial cell subsets highlighted Basal_I as exhibiting the highest number and intensity of intercellular interactions among all subtypes (Fig. 4A, B). Basal_I demonstrated intricate communication with other epithelial cell subsets through multiple ligand-receptor pairs, including Wnt5a-Fzd6, THBS1-SDC4/Sdc1/Cd47, Lamb3-Dag1/Cd44, Jag2-Notch1, F11-F11r, and Agrn-Dag1 (Fig. 4C). In various malignancies such as melanoma and gastric cancer, upregulation of WNT5a has been associated with heightened cancer cell migration and metastasis, mediated by the activation of protein kinase C (PKC) and WNT/calcium pathways. Similarly, Fzd6 activation has been linked to WNT/calcium pathways and PKC activation, frequently observed in glioblastomas, suggesting a potential synergy in driving tumor migration and invasion [45]. THBS1, a multifunctional glycoprotein, regulates extracellular matrix structure, cell–cell interactions, and physiological processes including vascular regulation, vasoconstriction, and tissue repair. Furthermore, THBS1 plays a significant role in immune regulation and tumor development [46]. Notably, elevated THBS1 expression has been associated with advanced stages of bladder cancer and poorer prognosis (Supplementary Fig. 1). LAMB3 has also been implicated in the invasiveness and metastatic potential of various cancers, including colon,

pancreatic, lung, cervical, gastric, and prostate cancers, underscoring its significance in cancer progression [47]. Interestingly, interactions involving Basal_I predominated in pathways associated with THBS, LAMININ, AGRN, and non-canonical WNT signaling (Fig. 4D), emphasizing the potential impact of Basal_I-mediated communication on tumor microenvironment dynamics and disease progression.

Tumor cells showed higher expression of specific transcription factors of Basal_I

The Monocle3 analysis revealed heightened expression of six transcription factors—Gata6, Nr3c1, Klf9, Egr1, Jun, and Nfix—in Basal_I. Statistical analysis confirmed that the expression levels of these transcription factors in Basal_I were significantly higher compared to other epithelial cell subtypes (Fig. 5A, B).

To further investigate, we analyzed mouse and human bladder cancer single-cell transcriptome data to discern differences in the expression of these transcription factors between bladder cancer cells and normal epithelial cells. In the human bladder cancer single-cell dataset, the expression levels of Gata6, Nr3c1, Klf9, Egr1, Jun, and Nfix were notably elevated in tumor cells compared to normal epithelial cells (Fig. 5C, D). Similarly, in the mouse bladder cancer single-cell dataset, tumor cells exhibited significantly higher expression levels of Egr1, Jun, and Nr3c1 compared to their normal epithelial counterparts (Fig. 5D, E). These findings suggest that these transcription factors are not only highly expressed in the transitional state of basal cells but also exhibit further elevation in expression levels in tumor cells. This underscores their potential significance in both normal epithelial cell differentiation processes and the pathogenesis of bladder cancer.

Subsequently, we conducted immunohistochemical staining on samples from both mouse bladder carcinoma in situ and human bladder cancer, juxtaposed with their respective normal bladder counterparts. The results revealed elevated Immunoreactive Assessment (IRA) scores for the aforementioned transcription factors in bladder cancer samples compared to normal bladder tissues, across both human and mouse specimens (Fig. 6). This consistent elevation in IRA scores further

(See figure on next page.)

Fig. 3 Pseudotemporal and SCENIC analysis identified Basal_I as transitional basal cell. **A** UMAP plot of epithelial cell differentiation colored by subtypes. **B** UMAP plot of epithelial cell differentiation colored by pseudotime. **C** 3D plot of epithelial cell differentiation colored by subtypes. **D** Density plot of epithelial cell along with pseudotime. **E** Heatmap of expression of gene profiles along with pseudotime. **F** Heatmap of expression of TFs along with pseudotime. **G** GO enrichment of cluster 2 (left) and 3 (right) in **F**. **H** Feature plot of six TFs expressed by subtypes. **I** Expression of six TFs along with pseudotime. **J** Heatmap of SCENIC outcomes. *DEGs* differentially expressed genes, *GO* gene ontology, *TFs* transcription factors

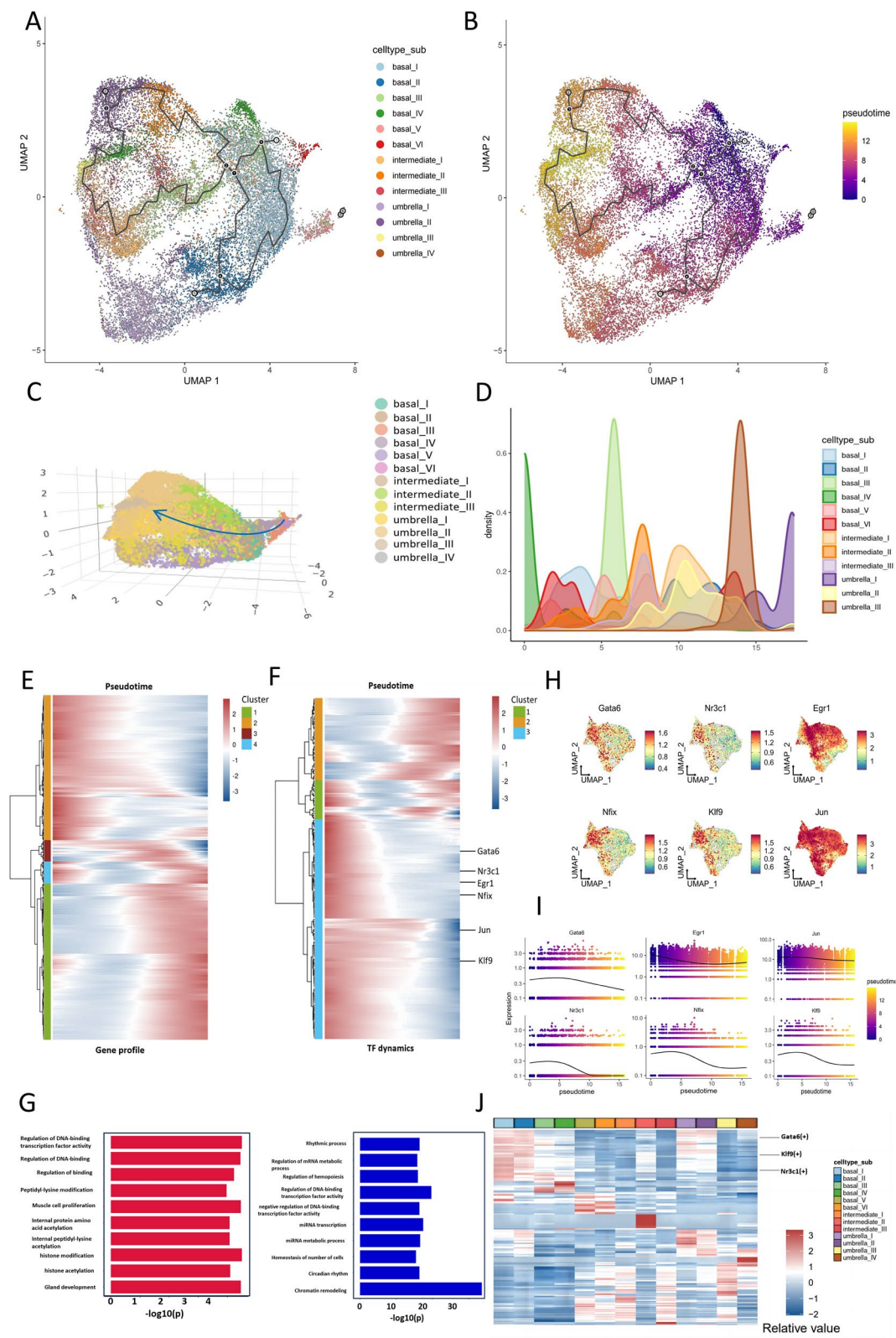


Fig. 3 (See legend on previous page.)

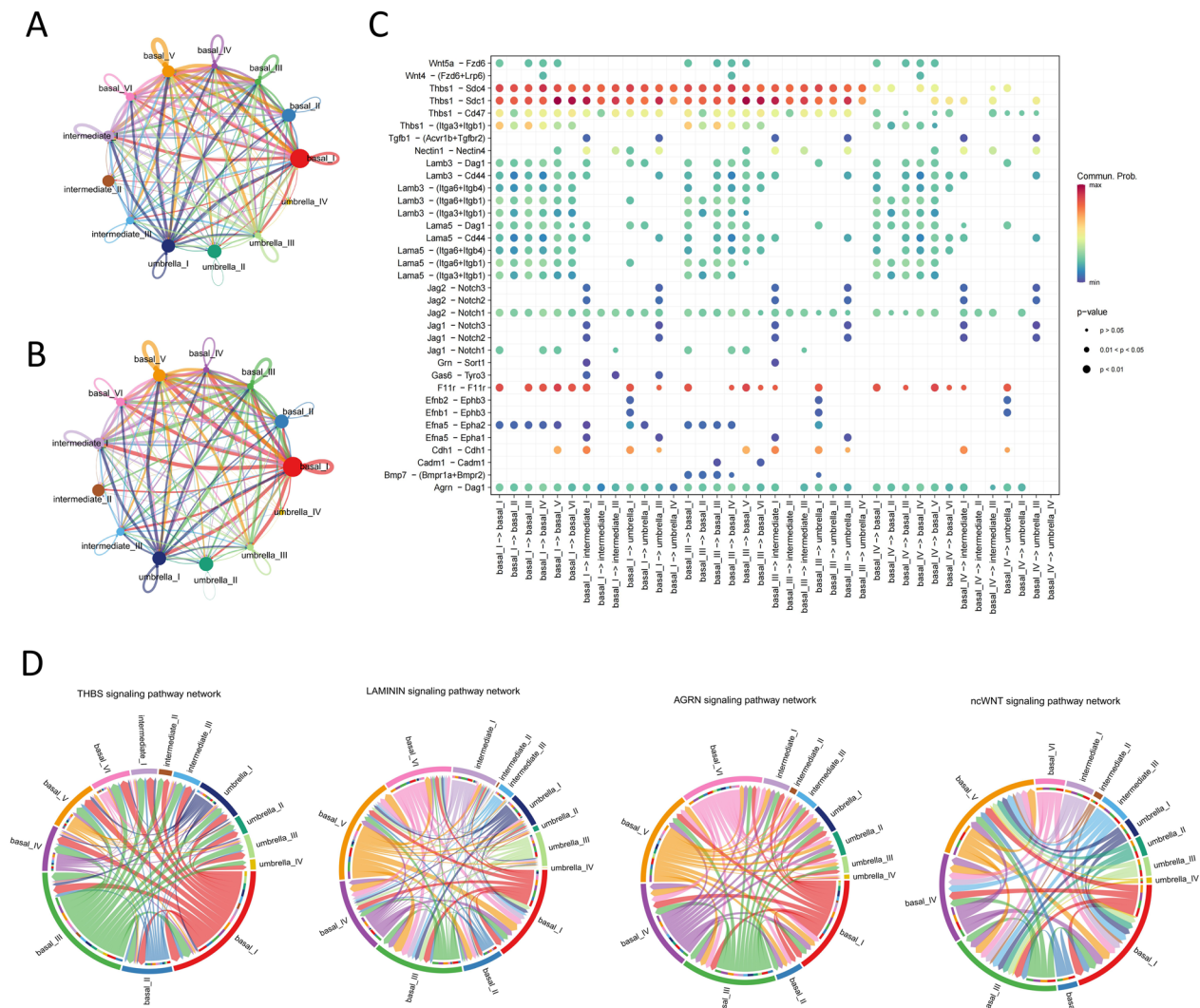


Fig. 4 Basal_I subtype dominated the interaction with other subtypes. **A** The number of cell communications between epithelial cell subpopulations. **B** The strength of cell communications between epithelial cell subpopulations. **C** Dotplot of ligand-receptor between epithelial cell subpopulations. **D** Chord plot of enriched pathways between epithelial cell subpopulations

substantiates the role of these transcription factors in bladder cancer pathogenesis and progression.

Key transcription factors are associated with the stage and prognosis of bladder cancer

In our exploration, we delved into the TCGA database to probe the relationship between the expression levels of the aforementioned six transcription factors and the stage and prognosis of bladder cancer. With the exception of NFIX, the expression levels of the remaining five transcription factors demonstrated a significant increase in patients with stage III and IV compared to those with stage II (Fig. 7A–F, left). Furthermore, patients exhibiting heightened expression of these transcription factors

experienced shorter survival durations (Fig. 7A–F, right). These findings underscore a direct correlation between the expression of these transcription factors and the progression of bladder cancer, with higher expression levels associated with advanced disease stages and poorer prognosis.

Discussion

Most bladder cancers originate from the urinary tract epithelium, though the precise cellular origin remains inconclusive. Despite advancements in surgical technology and the advent of immunotherapies, bladder cancer is still one of the important problems plaguing human health. The molecular mechanism of bladder cancer

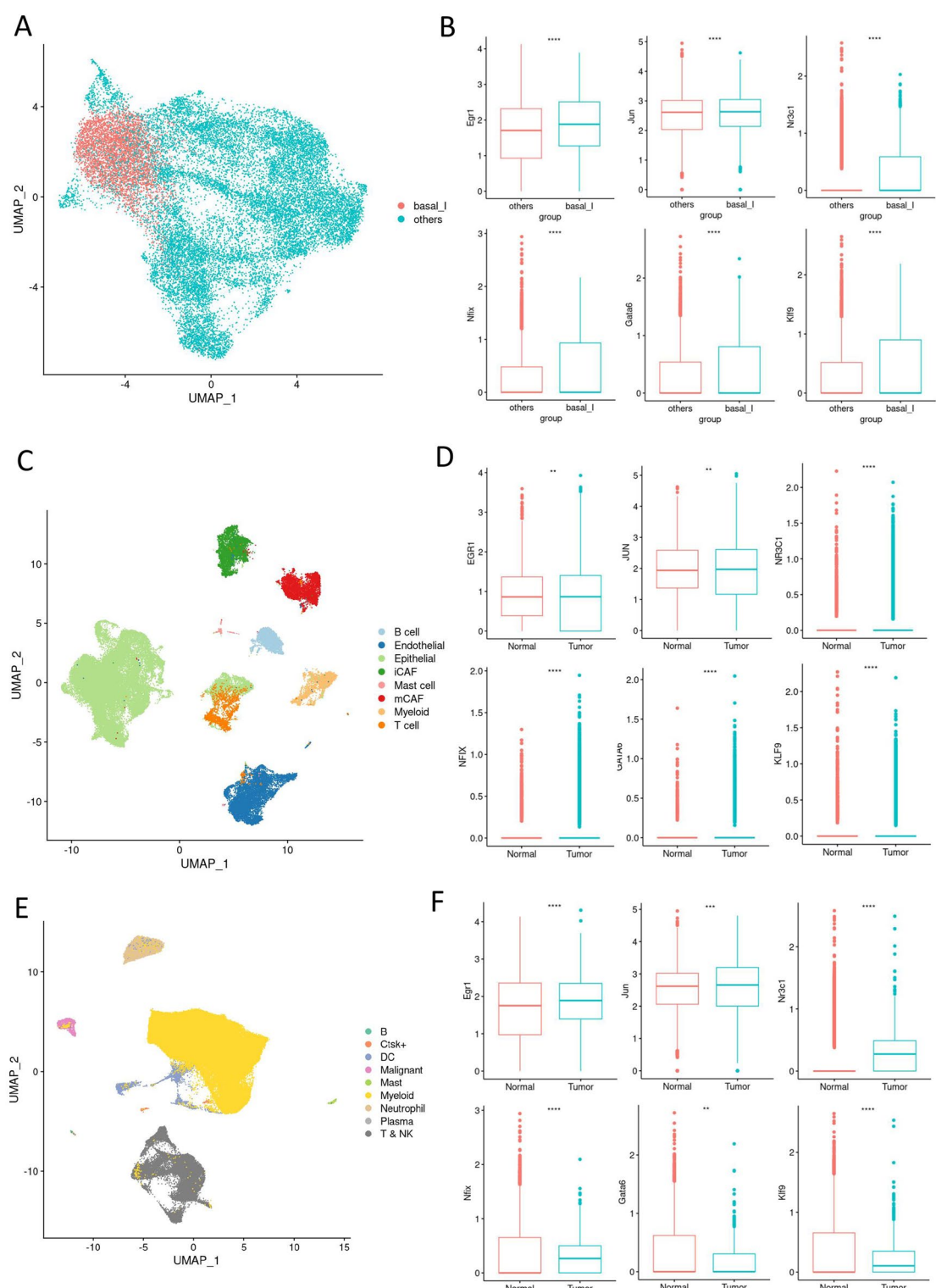


Fig. 5 Tumor cells showed higher expression of specific transcription factors of Basal_I. **A** Umap plot of normal mouse bladder cells grouped by basal_I and others. **B** Box plot of expression of six TFs grouped by basal_I and others. **C** Umap plot of human bladder cancer and adjacent normal cells grouped by major cell types. **D** Box plot of expression of six TFs grouped by human bladder cancer and adjacent normal cells. **E** Umap plot of mouse bladder cancer cells grouped by major cell types. **F** Box plot of expression of six TFs grouped by mouse bladder cancer and normal cells

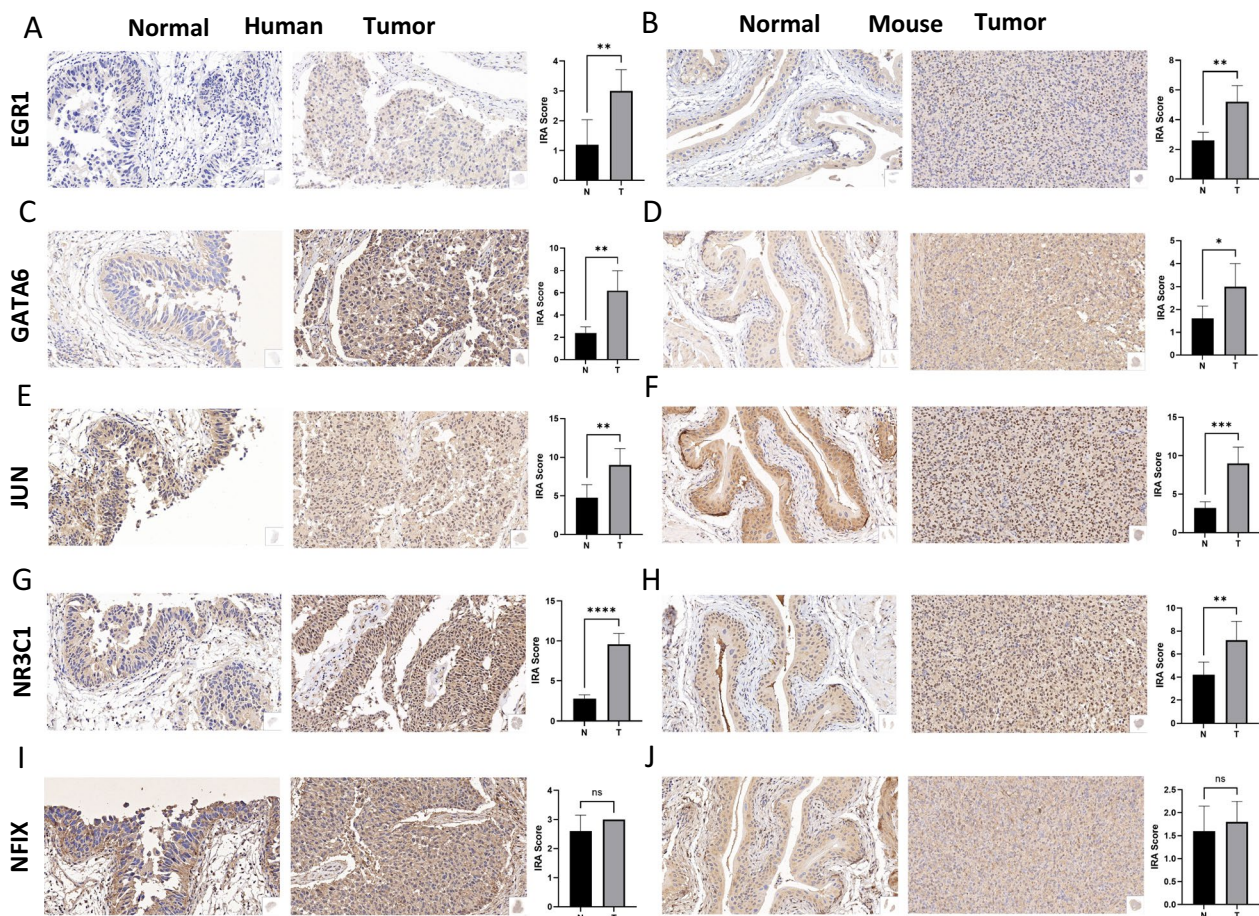


Fig. 6 IHC staining of key TFs in bladder cancer and normal samples. **A** IHC staining of EGR1 in human bladder cancer and normal samples. **B** IHC staining of EGR1 in mouse bladder cancer and normal samples. **C** IHC staining of GATA6 in human bladder cancer and normal samples. **D** IHC staining of GATA6 in mouse bladder cancer and normal samples. **E** IHC staining of JUN in human bladder cancer and normal samples. **F** IHC staining of JUN in mouse bladder cancer and normal samples. **G** IHC staining of NR3C1 in human bladder cancer and normal samples. **H** IHC staining of NR3C1 in mouse bladder cancer and normal samples. **I** IHC staining of NFIX in human bladder cancer and normal samples. **J** IHC staining of NFIX in mouse bladder cancer and normal samples

occurrence, progression and metastasis are still not fully understood [48].

Previous studies have primarily focused on identifying new subsets and their marker genes, or the construction of single-cell transcriptome profiles of normal bladder, without directly linking these analyses to bladder cancer. As a result, the available data have not been fully leveraged. By reintegrating these datasets, we identified a basal cell subset and key transcription factors potentially involved in the development of bladder cancer, which were not previously reported.

This study performed a comprehensive single-cell transcriptomic analysis of the normal mouse bladder, offering valuable insights into its cellular composition, functional heterogeneity, and the underlying mechanisms of bladder cancer progression. Our findings enrich existing knowledge of bladder biology

and highlight the importance of detailed cellular and molecular characterization in understanding normal tissue homeostasis and disease states.

By integrating three single-cell transcriptome datasets and applying the Harmony algorithm, we effectively mitigated the batch effect and identified 14 distinct cell clusters in a normal mouse bladder. Based on established markers, these clusters of cells are categorized as epithelial, stromal, and immune cells. Detailed analysis of epithelial cells revealed 13 subtypes, with Basal_I, Basal_III, and Basal_IV enriched in pathways associated with RNA splicing, mRNA processing, and DNA replication, indicating their proliferative and stem-like properties. These features are essential for tissue regeneration and homeostasis, highlighting the significance of these subtypes in bladder epithelial biology.

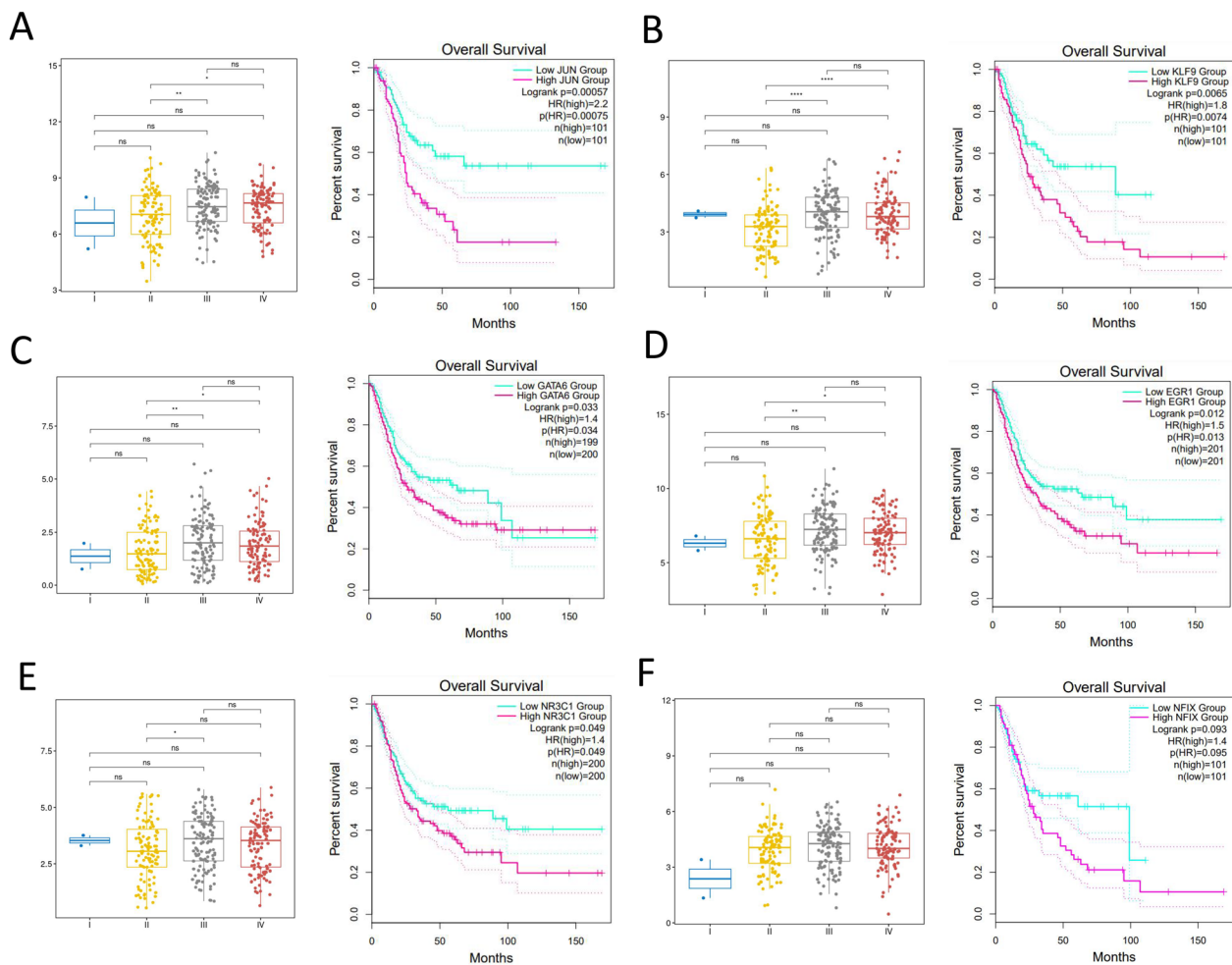


Fig. 7 Key transcription factors are associated with the stage and prognosis of bladder cancer. **A** Box plot of expression of JUN with stages and survival curve of patients with differentially expressed JUN. **B** Box plot of expression of KLF9 with stages and survival curve of patients with differentially expressed KLF9. **C** Box plot of expression of GATA6 with stages and survival curve of patients with differentially expressed GATA6. **D** Box plot of expression of EGR1 with stages and survival curve of patients with differentially expressed EGR1. **E** Box plot of expression of NR3C1 with stages and survival curve of patients with differentially expressed NR3C1. **F** Box plot of expression of NFIX with stages and survival curve of patients with differentially expressed NFIX

We performed pseudo-temporal analysis using Monocle3 to map the developmental trajectory from basal cells to intermediate cells and ultimately to umbrella cells, mirroring the differentiation hierarchy observed in other epithelial tissues. This trajectory supports the notion that Basal_I acts as an intermediate transition state, playing a pivotal role in the differentiation of basal cells into more specialized epithelial cell types. The elevated expression of transcription factors—Gata6, Nr3c1, Klf9, Egr1, Jun and Nfix—in Basal_I further emphasizes the importance of its regulatory function. These transcription factors likely facilitate the transition from basal cells to intermediate cells and umbrella cells, orchestrating the complex gene expression changes required for differentiation. This

hierarchical organization and the specific roles of these transcription factors align with established knowledge of epithelial biology and provide a framework for understanding bladder epithelial cell differentiation. It has been reported that GATA6 is highly expressed in stem-cell-enriched bladder cancer compared with stem-cell-deficient bladder cancer, sarcomatoid uroepithelial bladder cancer has a higher expression of NR3C1 than conventional uroepithelial bladder cancer, KLF9/RGS2 mediates bladder cancer progression, EGR1 and NFIX are involved in bladder cancer metastasis, and JUN contributes to bladder cancer immune escape [49–54]. By combining our previously generated dataset, we found that these transcription factors are further upregulated in tumor

cells [40, 41]. Immunohistochemical staining of mouse and human bladder cancer samples further validated these results, confirming the heightened expression of these transcription factors in bladder cancer.

CellChat analysis revealed that Basal_I exhibited the highest number and intensity of cell-to-cell interactions in the epithelial subtypes. Notably, interactions such as Wnt5a-Fzd6 pairs are involved in activating the WNT/calcium pathway and PKC, both of which are implicated in cancer cell migration and metastasis [45]. Additionally, elevated expression of THBS1 has been linked to advanced and poorer prognosis of bladder cancer, highlighting its potential role in tumor progression [46]. The extensive interactions involving interactions Basal_I with other subtypes suggest that Basal_I may play a key role in regulating the tumor microenvironment, thereby influencing cancer progression.

Using the TCGA database, we examined the relationship between the expression of six transcription factors and the stage and prognosis of bladder cancer. With the exception of NFIX, the expression of the remaining transcription factors was significantly higher in stage III and IV patients than in stage II patients. Higher expression levels are associated with shorter survival, suggesting that these transcription factors may be potential biomarkers for advanced bladder cancer and poor prognosis.

Conclusion

In conclusion, our comprehensive analysis elucidates the complex cellular structure and functional heterogeneity of the normal mouse bladder and found a transitional state of basal cells, which may be related to the occurrence and development of bladder cancer. Future studies should focus on validating these findings in human tissues and exploring the therapeutic potential of targeting these pathways and transcription factors in bladder cancer.

Abbreviations

BC	Bladder cancer
NMIBC	Non-muscle-invasive bladder cancer
MIBC	Muscle-invasive bladder cancer
ScRNA-seq	Single-cell RNA sequencing
GO	Gene ontology
TF	Transcription factor
PKC	Protein kinase C
IRA	Immunoreactive assessment
WT	Wild-type
BCMVN	Mean-variance-normalized bimodality coefficient
DEGs	Differentially expressed genes
GEO	Gene Expression Omnibus
UMAP	Uniform manifold approximation and projection

Supplementary Information

The online version contains supplementary material available at <https://doi.org/10.1186/s12967-024-05841-0>.

Supplementary Material 1.

Acknowledgements

We thank all the authors who contributed to this topic.

Author contributions

Study conception and design, Y.H and K.C.; performed experiments or data collection, J.H., L.L., and Z.L.; computational and statistical analyses, Y.L. and Y.D.; writing—original drafts, Y.L., P.S., Y.D. and Z.Y.; writing—review and editing, P.S., Y.K., and J.L.

Funding

This research was supported by the National Natural Science Foundation of China (No. 82303623), the National Sponsored Postdoctoral Research Program of China (No. GZB20230243), the China Postdoctoral Science Foundation (No. 2023M731199), the Postdoctoral Innovation Research Position of Hubei Province, China (Postdoctoral No. 331048), the Fundamental Research Funds for Central Universities (No. YCJJ20241411), and the Tongji Hospital of Tongji Medical College, Huazhong University of Science and Technology, China (2022YBJ018, 2021RCYJ005).

Availability of data and materials

The progressed scRNA sequencing data of normal mouse bladder was downloaded from Gene Expression Omnibus (GEO) database including GSE163029, GSM3723360 and GSM3723361. The raw scRNA sequencing data of bladder cancer patients are available in the GSA-Human database under the accession code HRA000212 and in the SRA datasets under BioProject PRJNA662018. The raw data of mouse bladder cancer are available in GEO under accession number GSE189127. The public TCGA-BLCA data used in this study are publically available under <http://xena.ucsc.edu/>.

Code availability

No custom code or software were generated in this work.

Declarations

Ethics approval and consent to participate

All procedures were approved by the Institutional Review Board of Tongji Medical College, Huazhong University of Science and Technology.

Consent for publication

Not applicable.

Competing interests

The authors declare no competing interests.

Author details

¹Department of Urology, Tongji Hospital, Tongji Medical College, Huazhong University of Science and Technology, Wuhan, China. ²Institute of Urology, Tongji Hospital, Tongji Medical College, Huazhong University of Science and Technology, Wuhan, China.

Received: 5 August 2024 Accepted: 31 October 2024

Published online: 10 November 2024

References

- Gvozden Rosic DSSO. Cancer signaling, cell/gene therapy, diagnosis and role of nanobiomaterials. *Adv Biol Earth Sci.* 2024;9:11–34. <https://doi.org/10.62476/abes9s11>.
- Miryusifova K. The saffron effects on the dynamics of experimental epilepsy. *Adv Biol Earth Sci.* 2024;9:196–202. <https://doi.org/10.62476/abes9196>.

3. Karadağ M. Use of *Prunus armeniaca* L. seed oil and pulp in health and cosmetic products. *Adv Biol Earth Sci.* 2024;9:105–10. <https://doi.org/10.62476/abess105>.
4. Imran Ali WAWK. Thalidomide: a banned drug resurged into future anti-cancer drug. *Curr Drug Ther.* 2012;7:13–23. <https://doi.org/10.2174/157488512800389164>.
5. Ali I, Wani WA, Saleem K, Wesselinova D. Syntheses, DNA binding and anticancer profiles of L-glutamic acid ligand and its Copper(II) and Ruthenium(III) complexes. *Med Chem.* 2013;9:11–21. <https://doi.org/10.2174/157340613804488297>.
6. Ali I, Alsehlhi M, Scotti L, Tullius Scotti M, Tsai S, Yu R, Hsieh MF, Chen J. Progress in polymeric nano-medicines for theranostic cancer treatment. *Polymers.* 2020;12:598. <https://doi.org/10.3390/polym12030598>.
7. Ali I, Wani WA, Saleem K, Hsieh M. Anticancer metallodrugs of glutamic acid sulphonamides: in silico, DNA binding, hemolysis and anticancer studies. *Rsc Adv.* 2014;4:29629–41. <https://doi.org/10.1039/C4RA02570A>.
8. Ali I, et al. Enantioselective toxicity and carcinogenesis. *Curr Pharm Anal.* 2005;1:109–25. <https://doi.org/10.2174/1573412052953328>.
9. Ali I, et al. Glutamic acid and its derivatives: candidates for rational design of anticancer drugs. *Future Med Chem.* 2013;5:961–78. <https://doi.org/10.2174/1573412052953328>.
10. Ali I, et al. Synthesis and synergistic antifungal activities of a pyrazoline based ligand and its Copper(II) and Nickel(II) complexes with conventional antifungals. *Microb Pathog.* 2012;53:66–73. <https://doi.org/10.1016/j.micpath.2012.04.005>.
11. Siegel RL, Miller KD, Wagle NS, Jemal A. Cancer statistics, 2023. *CA Cancer J Clin.* 2023;73:17–48. <https://doi.org/10.3322/caac.21763>.
12. Grayson M. Bladder cancer. *Nature.* 2017;551:S33. <https://doi.org/10.1038/551S33a>.
13. Burger M, Catto JW, Dalbagni G, et al. Epidemiology and risk factors of urothelial bladder cancer. *Eur Urol.* 2013;63:234–41. <https://doi.org/10.1016/j.eururo.2012.07.033>.
14. Robertson AG, Kim J, Al-Ahmadie H, et al. Comprehensive molecular characterization of muscle-invasive bladder cancer. *Cell.* 2017;171:540–56. <https://doi.org/10.1016/j.cell.2017.09.007>.
15. Chou R, Selph SS, Buckley DI, Gustafson KS, Griffin JC, Grusing SE, Gore JL. Treatment of muscle-invasive bladder cancer: a systematic review. *Cancer.* 2016;122:842–51. <https://doi.org/10.1002/cncr.29843>.
16. Ghandour R, Singla N, Lotan Y. Treatment options and outcomes in non-metastatic muscle invasive bladder cancer. *Trends Cancer.* 2019;5:426–39. <https://doi.org/10.1016/j.trecan.2019.05.011>.
17. Foxman B. The epidemiology of urinary tract infection. *Nat Rev Urol.* 2010;7:653–60. <https://doi.org/10.1038/nrurol.2010.190>.
18. Suva ML, Tirosh I. Single-cell RNA sequencing in cancer: lessons learned and emerging challenges. *Mol Cell.* 2019;75:7–12. <https://doi.org/10.1016/j.molcel.2019.05.003>.
19. Kulkarni A, Anderson AG, Merullo DP, Konopka G. Beyond bulk: a review of single cell transcriptomics methodologies and applications. *Curr Opin Biotechnol.* 2019;58:129–36. <https://doi.org/10.1016/j.copbio.2019.03.001>.
20. Gohil SH, Iorgulescu JB, Braun DA, Keskin DB, Livak KJ. Applying high-dimensional single-cell technologies to the analysis of cancer immunotherapy. *Nat Rev Clin Oncol.* 2021;18:244–56. <https://doi.org/10.1038/s41571-020-00449-x>.
21. Zheng L, Qin S, Si W, et al. Pan-cancer single-cell landscape of tumor-infiltrating T cells. *Science.* 2021;374: e6474. <https://doi.org/10.1126/science.abe6474>.
22. Cheng S, Li Z, Gao R, et al. A pan-cancer single-cell transcriptional atlas of tumor infiltrating myeloid cells. *Cell.* 2021;184:792–809. <https://doi.org/10.1016/j.cell.2021.01.010>.
23. Luo H, Xia X, Huang L, et al. Pan-cancer single-cell analysis reveals the heterogeneity and plasticity of cancer-associated fibroblasts in the tumor microenvironment. *Nat Commun.* 2022. <https://doi.org/10.1038/s41467-022-34395-2>.
24. Lai H, Cheng X, Liu Q, et al. Single-cell RNA sequencing reveals the epithelial cell heterogeneity and invasive subpopulation in human bladder cancer. *Int J Cancer.* 2021;149:2099–115. <https://doi.org/10.1002/ijc.33794>.
25. Gouin KR, Ing N, Plummer JT, et al. An N-Cadherin 2 expressing epithelial cell subpopulation predicts response to surgery, chemotherapy and immunotherapy in bladder cancer. *Nat Commun.* 2021;12:4906. <https://doi.org/10.1038/s41467-021-25103-7>.
26. Wang L, Sfakianos JP, Beaumont KG, et al. Myeloid cell-associated resistance to PD-1/PD-L1 blockade in urothelial cancer revealed through bulk and single-cell RNA sequencing. *Clin Cancer Res.* 2021;27:4287–300. <https://doi.org/10.1158/1078-0432.CCR-20-4574>.
27. Hu J, Othmane B, Yu A, Li H, Cai Z, Chen X, Ren W, Chen J, Zu X. 5mC regulator-mediated molecular subtypes depict the hallmarks of the tumor microenvironment and guide precision medicine in bladder cancer. *BMC Med.* 2021;19:289. <https://doi.org/10.1186/s12916-021-02163-6>.
28. Lee HW, Chung W, Lee HO, et al. Single-cell RNA sequencing reveals the tumor microenvironment and facilitates strategic choices to circumvent treatment failure in a chemorefractory bladder cancer patient. *Genome Med.* 2020;12:47. <https://doi.org/10.1186/s13073-020-00741-6>.
29. Li Y, Liu Y, Gao Z, et al. Single-cell transcriptomes of mouse bladder urothelium uncover novel cell type markers and urothelial differentiation characteristics. *Cell Prolif.* 2021;54: e13007. <https://doi.org/10.1111/cpr.13007>.
30. Yu Z, Liao J, Chen Y, et al. Single-cell transcriptomic map of the human and mouse bladders. *J Am Soc Nephrol.* 2019;30:2159–76. <https://doi.org/10.1681/ASN.2019040335>.
31. Yuen J, Mak D, Chan ES, Gohel M, Ng CF. Tumor inhibitory effects of intravesical ganoderma lucidum instillation in the syngeneic orthotopic MB49/C57 bladder cancer mice model. *J Ethnopharmacol.* 2018;223:113–21. <https://doi.org/10.1016/j.jep.2018.05.020>.
32. Remmele W, Stegner HE. Recommendation for uniform definition of an immunoreactive score (IRS) for immunohistochemical estrogen receptor detection (ER-ICA) in breast cancer tissue. *Pathologe.* 1987;8:138–40.
33. Butler A, Hoffman P, Smibert P, Papalexi E, Satija R. Integrating single-cell transcriptomic data across different conditions, technologies, and species. *Nat Biotechnol.* 2018;36:411–20. <https://doi.org/10.1038/nbt.4096>.
34. McGinnis CS, Murrow LM, Gartner ZJ. DoubletFinder: doublet detection in single-cell RNA sequencing data using artificial nearest neighbors. *Cell Syst.* 2019;8:329–37. <https://doi.org/10.1016/j.cels.2019.03.003>.
35. Korsunsky I, Millard N, Fan J, et al. Fast, sensitive and accurate integration of single-cell data with harmony. *Nat Methods.* 2019;16:1289–96. <https://doi.org/10.1038/s41592-019-0619-0>.
36. Becht E, McInnes L, Healy J, Dutertre CA, Kwok I, Ng LG, Ginhoux F, Newell EW. Dimensionality reduction for visualizing single-cell data using UMAP. *Nat Biotechnol.* 2018. <https://doi.org/10.1038/nbt.4314>.
37. Yu G, Wang LG, Han Y, He QY. clusterProfiler: an R package for comparing biological themes among gene clusters. *OMICS.* 2012;16:284–7. <https://doi.org/10.1089/omi.2011.0118>.
38. Cao J, Spielmann M, Qiu X, et al. The single-cell transcriptional landscape of mammalian organogenesis. *Nature.* 2019;566:496–502. <https://doi.org/10.1038/s41586-019-0969-x>.
39. Jin S, Guerrero-Juarez CF, Zhang L, Chang I, Ramos R, Kuan CH, Myung P, Plikus MV, Nie Q. Inference and analysis of cell–cell communication using CellChat. *Nat Commun.* 2021;12:1088. <https://doi.org/10.1038/s41467-021-21246-9>.
40. Liu L, Hou Y, Deng C, Tao Z, Chen Z, Hu J, Chen K. Single cell sequencing reveals that CD39 inhibition mediates changes to the tumor micro-environment. *Nat Commun.* 2022;13:6740. <https://doi.org/10.1038/s41467-022-34495-z>.
41. Chen Z, Zhou L, Liu L, Hou Y, Xiong M, Yang Y, Hu J, Chen K. Single-cell RNA sequencing highlights the role of inflammatory cancer-associated fibroblasts in bladder urothelial carcinoma. *Nat Commun.* 2020;11:5077. <https://doi.org/10.1038/s41467-020-18916-5>.
42. Chen X, Qiu H, Wang C, Yuan Y, Tickner J, Xu J, Zou J. Molecular structure and differential function of choline kinases CHKalpha and CHKbeta in musculoskeletal system and cancer. *Cytokine Growth Factor Rev.* 2017;33:65–72. <https://doi.org/10.1016/j.cytogr.2016.10.002>.
43. Sallmyr A, Bhandari SK, Naila T, Tomkinson AE. Mammalian DNA ligases; roles in maintaining genome integrity. *J Mol Biol.* 2024;436: 168276. <https://doi.org/10.1016/j.jmb.2023.168276>.
44. Fritzler MJ, Rattner JB, Luft LM, Edworthy SM, Casiano CA, Peebles C, Mahler M. Historical perspectives on the discovery and elucidation of autoantibodies to centromere proteins (CENP) and the emerging importance of antibodies to CENP-F. *Autoimmun Rev.* 2011;10:194–200. <https://doi.org/10.1016/j.autrev.2010.09.025>.
45. Corda G, Sala A. Non-canonical WNT/PCP signalling in cancer: Fzd6 takes centre stage. *Oncogenesis.* 2017;6: e364. <https://doi.org/10.1038/oncsis.2017.69>.

46. Kaur S, Bronson SM, Pal-Nath D, Miller TW, Soto-Pantoja DR, Roberts DD. Functions of thrombospondin-1 in the tumor microenvironment. *Int J Mol Sci.* 2021;22:4570. <https://doi.org/10.3390/ijms22094570>.
47. Zhang H, Pan YZ, Cheung M, Cao M, Yu C, Chen L, Zhan L, He ZW, Sun CY. LAMB3 mediates apoptotic, proliferative, invasive, and metastatic behaviors in pancreatic cancer by regulating the PI3K/Akt signaling pathway. *Cell Death Dis.* 2019;10:230. <https://doi.org/10.1038/s41419-019-1320-z>.
48. Tran L, Xiao JF, Agarwal N, Duex JE, Theodorescu D. Advances in bladder cancer biology and therapy. *Nat Rev Cancer.* 2021;21:104–21. <https://doi.org/10.1038/s41568-020-00313-1>.
49. Yang Z, Chen J, Xie H, Liu T, Chen Y, Ma Z, Pei X, Yang W, Li L. Androgen receptor suppresses prostate cancer metastasis but promotes bladder cancer metastasis via differentially altering miRNA525-5p/SLPI-mediated vasculogenic mimicry formation. *Cancer Lett.* 2020;473:118–29. <https://doi.org/10.1016/j.canlet.2019.12.018>.
50. Tang C, Ma J, Liu X, Liu Z. Development and validation of a novel stem cell subtype for bladder cancer based on stem genomic profiling. *Stem Cell Res Ther.* 2020;11:457. <https://doi.org/10.1186/s13287-020-01973-4>.
51. Ni Z, Sun P, Zheng J, et al. JNK signaling promotes bladder cancer immune escape by regulating METTL3-mediated m⁶A modification of PD-L1 mRNA. *Cancer Res.* 2022;82:1789–802. <https://doi.org/10.1158/0008-5472.CAN-21-1323>.
52. Xu XH, Sun JM, Chen XF, Zeng XY, Zhou HZ. MicroRNA-494-3p facilitates the progression of bladder cancer by mediating the KLF9/RGS2 axis. *Kaohsiung J Med Sci.* 2022;38:1070–9. <https://doi.org/10.1002/kjm2.12588>.
53. Ren L, Jiang M, Xue D, et al. Nitroxoline suppresses metastasis in bladder cancer via EGR1/circNDRG1/miR-520h/smad7/EMT signaling pathway. *Int J Biol Sci.* 2022;18:5207–20. <https://doi.org/10.7150/ijbs.69373>.
54. Garioni M, Tschan VJ, Blukacz L, et al. Patient-derived organoids identify tailored therapeutic options and determinants of plasticity in sarcomatoid urothelial bladder cancer. *NPJ Precis Oncol.* 2023;7:112. <https://doi.org/10.1038/s41698-023-00466-w>.

Publisher's Note

Springer Nature remains neutral with regard to jurisdictional claims in published maps and institutional affiliations.